World Journal of Gastroenterology

Online Submissions: http://www.wjgnet.com/1007-9327office
wjg@wjgnet.com
doi:10.3748/wjg.v16.i17.2109

World J Gastroenterol 2010 May 7; 16(17): 2109-2119
ISSN 1007-9327 (print)

ORIGINAL ARTICLE

Differentiation of focal liver lesions using three-dimensional ultrasonography: Retrospective and prospective studies

Wen Luo, Kazushi Numata, Manabu Morimoto, Akito Nozaki, Michio Ueda, Masaaki Kondo, Satoshi Morita, Katsuaki Tanaka

Wen Luo, Kazushi Numata, Manabu Morimoto, Akito Nozaki, Michio Ueda, Masaaki Kondo, Katsuaki Tanaka, Gastroenterological Center, Yokohama City University Medical Center, 4-57 Urafune-cho, Minami-ku, Yokohama, Kanagawa 232-0024, Japan
Wen Luo, Department of Ultrasound, Xijing Hospital, Fourth Military Medical University, 15th Changle Xi Road, Xi'an 710032, Shaanxi Province, China
Satoshi Morita, Department of Biostatistics and Epidemiology, Yokohama City University Medical Center, 4-57 Urafune-cho, Minami-ku, Yokohama, Kanagawa 232-0024, Japan
Author contributions: Luo W and Numata K designed the research; Numata K and Morimoto M performed the research; Luo W, Nozaki A, Kondo M and Tanaka K contributed analytic tools; Luo W, Numata K, Ueda M and Morita S analyzed the data; Luo W and Numata K wrote the paper.
Correspondence to: Kazushi Numata, MD, Gastroenterological Center, Yokohama City University Medical Center, 4-57 Urafune-cho, Minami-ku, Yokohama, Kanagawa 232-0024, Japan. kz-numa@urahp.yokohama-cu.ac.jp
Telephone: +81-45-2615656 Fax: +81-45-2619492
Received: November 24, 2009 Revised: January 6, 2010
Accepted: January 13, 2010
Published online: May 7, 2010

Abstract

AIM: To differentiate focal liver lesions based on enhancement patterns using three-dimensional ultrasonography (3D US) with perflubutane-based contrast agent.

METHODS: Two hundred and eighty two patients with focal liver lesions, including 168 hepatocellular carcinomas (HCCs), 63 metastases, 40 hemangiomas and 11 focal nodular hyperplasias (FNHs), were examined by 3D US with perflubutane-based contrast agent. Tomographic ultrasound images and sonographic angiograms were reconstructed. Among 282 lesions, enhancement patterns of 163 lesions between January 2007 and October 2007 were analyzed retrospectively. Then from November 2007 to May 2008, compared with contrast-enhanced (CE) 2D US, CE 3D US was performed on 119 lesions for prospective differential diagnosis. Sensitivity, specificity, area under receiver operating characteristic curve (A_z) and inter-reader agreement were assessed.

RESULTS: With the tridimensional view, dominant enhancement patterns were revealed as diffuse enhancement or peripheral ring-like enhancement, followed with washout change for HCCs or metastases, respectively, and peripheral nodular enhancement or diffuse enhancement with spoke-wheel arteries, followed by persistent enhancement for hemangiomas or FNHs, respectively. At CE 3D US, the prospective differentiation of lesions showed sensitivity 92% (mean for two readers), specificity 91% and A_z value 0.95 for HCCs, 84%, 97%, and 0.95 for metastases, 91%, 98%, and 0.98 for hemangiomas and 80%, 99%, and 0.99 for FNHs, respectively, while good to excellent inter-reader agreement was achieved. No significant difference exists between prospective diagnosis accuracy at CE 3D US and that at CE 2D US.

CONCLUSION: CE 3D US provides a spatial perspective for liver tumor enhancement, and could help in differentiating focal liver lesions.

Key words: Three-dimensional; Ultrasonography; Contrast agent; Liver; Neoplasms

Peer reviewer: Mirko D'Onofrio, MD, Assistant Professor, Department of Radiology, GB Rossi University Hospital, University of Verona, Piazzale LA Scuro 10, Verona, 37134, Italy

Luo W, Numata K, Morimoto M, Nozaki A, Ueda M, Kondo M, Morita S, Tanaka K. Differentiation of focal liver lesions using

three-dimensional ultrasonography: Retrospective and prospective studies. *World J Gastroenterol* 2010; 16(17): 2109-2119 Available from: URL: http://www.wjgnet.com/1007-9327/full/v16/i17/2109.htm DOI: http://dx.doi.org/10.3748/wjg.v16.i17.2109

INTRODUCTION

Focal liver lesions are increasingly being discovered with the widespread use of diagnostic imaging modalities, and differentiation of various liver lesions is considered to be critical for determining treatment options. Tremendous advancements in imaging techniques, including ultrasonography (US), computed tomography (CT), and magnetic resonance imaging (MRI) have resulted in these modalities being accepted as effective and thus widely used to characterize focal liver lesions[1-5]. This reduces the necessity of invasive histopathological examination.

With the advantages of non-invasiveness, no radiation and flexible operation, contrast-enhanced (CE) US has become increasingly important in the detection and characterization of focal liver tumors over the past several years[6-13]. Microbubbles of ultrasound contrast agent approximately the same size as red blood cells move into vessels but not through the vascular endothelium into the interstitium, which provides exact information about vascularity by reflecting specific signals, while some contrast agents present a postvascular hepato-specific phase probably due to reticuloendothelial system phagocytosis or the adherence of microbubbles to hepatic sinusoids[14-17]. Sonazoid (Daiichi Sankyo, Tokyo, Japan), a newly-developed second-generation ultrasound contrast agent, which consists of microbubbles (mean diameter 2-3 μm) of a perfluorobutane gas stabilized by a phospholipid monolayer shell, allows continuous real-time CE imaging for more than 10 min, and improves the reproducibility and durability of CE US examination[18-20].

Recently, the advent of CE three-dimensional (3D) US, facilitating demonstration of the desired regions with dynamic information in spatial volume, has led to new applications of CE US imaging[21-24]. Different from the 2D images, CE 3D US acquires the data in a volume of interest (VOI) by automatically scanning with a desired angle and allows reconstruction of tomographic images in three orthogonal planes and rendered angiogram-like images. With the feature of illustration in three dimensions, CE 3D US has been proven to offer accurate and detailed visualization of the vascular characteristics of various focal liver tumors[25,26].

To our knowledge, although many studies on differentiation among various focal liver lesions have been conducted using CE 2D US[27-29] and recently a few using CE 2D US with Sonazoid[30], the exact value of CE 3D US with Sonazoid in the differential diagnosis of various focal liver lesions has not yet been clarified. Thus, in this study, in order to examine the potential role of CE 3D US in characterizing focal liver lesions, we retrospectively evaluated the enhancement patterns and the diagnostic criteria established using dominant enhancement patterns were then applied to differentiation among focal liver lesions in a prospective study.

MATERIALS AND METHODS

Patients

Institutional Review Board approval was obtained for this retrospective and prospective study and informed consent was obtained from all patients. The reference standards for focal liver lesions in this study were described as follows: hepatocellular carcinomas (HCCs) with diameters exceeding 2 cm were confirmed by typical findings on both dynamic multi-detector CT and CE MRI[31]; HCCs exceeding 2 cm in diameter without typical radiological findings and those less than 2 cm in diameter, as well as all the liver metastases, were confirmed using histopathological results from percutaneous biopsy or surgery; benign tumors were confirmed by typical appearance on either dynamic multi-detector CT or CE MRI with at least 6-mo follow-up by dynamic multi-detector CT or CE MRI, and those without typical findings were confirmed histopathologically.

Between January 2007 and October 2007, 183 consecutive patients known or suspected to have focal liver lesions were examined using CE 3D US. Among these, 163 patients (90 men and 73 women) with 163 focal liver tumors were retrospectively identified, based on the following enrollment criteria: satisfactory CE 3D US images were acquired without artifacts from the cardiac and respiratory motion, shadows of costal bones, and abdominal gas; the definitive diagnosis of lesions was confirmed according to reference standards; the lesions had not been treated previously. Twenty patients were excluded: 6 with HCCs and 6 with hepatic metastasis lesions lacking a histological diagnosis; 3 HCCs and 3 hemangiomas with serious artifacts on the images; 2 benign lesions suspected on clinical information and imaging follow-up, without typical radiological findings and histological results. For 58 patients with multiple lesions, only the largest one with CE 3D US images and confirmed diagnosis was selected for evaluation. These 163 lesions were reviewed in the retrospective study to summarize the dominant enhancement patterns, which would be the diagnostic criteria in the prospective study.

From November 2007 to May 2008, the prospective study was conducted using CE 3D US on 124 consecutive patients with suspicious focal liver lesions detected by prior conventional US or CT and after that, CE 2D US was performed on each patient. For 40 patients with multiple lesions, CE 3D US examination was performed on the largest one, and if the largest lesion was not suitable for scanning due to its location, the next largest lesion was selected. CE 2D US was performed on the same lesion scanned by CE 3D US. In the prospective study, the exclusion criteria were: patients unable to hold breath; lesions with inappropriate locations for acquiring CE 3D

Table 1 Clinical characteristics of patients and focal liver lesions in retrospective and prospective studies (mean ± SD)

	Retrospective study (n = 163)				Prospective study (n = 119)			
	HCC	Metastasis	Hemangioma	FNH	HCC	Metastasis	Hemangioma	FNH
No. of patients	98	35	24	6	70	28	16	5
No. of lesions	98	35	24	6	70	28	16	5
Age of patients (yr)	69.8 ± 6.5	64.8 ± 13.2	58.9 ± 11.2	54.2 ± 16.7	72.5 ± 7.3	69.2 ± 8.3	55.4 ± 14.1	52.8 ± 18.4
Liver cirrhosis								
Child-Pugh class A	78	0	1	0	52	0	0	0
Child-Pugh class B	20	0	0	0	18	0	0	0
Lesion diameter (mm)	30.1 ± 24.3	28.9 ± 15.5	31.5 ± 18.0	38.4 ± 12.0	29.1 ± 20.4	30.7 ± 21.1	33.7 ± 16.7	37.4 ± 15.0
Final diagnosis								
Surgery	11	15	2	0	6	12	0	0
Biopsy	29	20	0	1	19	16	0	1
Radiological imaging	58	0	22	5	45	0	16	4

HCC: Hepatocellular carcinoma; FNH: Focal nodular hyperplasia.

US images due to artifacts from costal bone shadows, heart motion or abdominal gas; patients with lesions requiring histopathological diagnosis according to a reference standard but in whom surgery or biopsy was not possible due to poor liver function or lack of consent. Finally, 119 patients (67 men and 52 women) with 119 liver lesions were enrolled, while 2 patients with HCCs less than 2 cm in diameter and one with metastases were excluded for lack of consent on biopsy, and one patient with HCC and one with hemangioma were excluded for the obstruction of costal bone shadow.

Final diagnosis and clinical characteristics are shown in Table 1. The metastases in the retrospective study included 17 from colon carcinomas, 6 from pancreatic carcinomas, 5 from intrahepatic cholangiocellular carcinomas (ICC), 4 from rectal carcinomas, 1 from an ileum carcinoma, 1 from a gallbladder carcinoma and 1 from an ovarian carcinoma. Metastases in the prospective study comprised 15 from colon carcinomas, 4 from pancreatic carcinomas, 4 ICCs, 2 from rectal carcinomas, 1 from an ileum carcinoma, 1 from an ovarian carcinoma, and 1 from a gastric carcinoma. In this study, we classified the ICCs as hepatic metastasis because differentiation of ICCs from metastasis is difficult using only radiological imaging enhancement patterns.

Data acquisition

In the retrospective study, using the LOGIQ 7 ultrasound imaging system and 4D3CL volume probe (GE Healthcare, Milwaukee, WI) with a 2.0-5.5 MHz frequency, CE 3D US was performed by one sonographer with 10 years experience in using abdominal CE US. In the prospective study, CE 3D US was performed by the same sonographer in the retrospective study. After 1 or 2 d using the LOGIQ 7 ultrasound imaging system and 3.5 CS convex probe (GE Healthcare, Milwaukee, WI), CE 2D US was performed on each lesion by the same sonographer at CE 3D US. In this study, the acquisition of 3D images was performed with a convex volume 4D3C-L probe which scans automatically with internal sectorial mechanical tilt movement to obtain the data. The scanning angle could be selected from 15° to 84°. In this study we used 30-70° depending on different tumor sizes and the duration for one scanning process varied from 4.5 to 21.3 s (mean time, 12 s).

Prior to both CE 2D US and CE 3D US scanning, all patients received an intravenous bolus injection of 0.2 mL Sonazoid followed by a 2 mL 5% glucose solution and subsequent infusion of 5% glucose solution at 10 mL/min. The coded harmonic angio (CHA) mode (mechanical index = 0.5-0.9) at 8 to 13 frames per second was used for both CE 2D US and CE 3D US scanning. The contrast sonography process included three phases, that is, an early phase (10-40 s after contrast medium injection), a middle phase (80-120 s after contrast medium injection) and a late phase (more than 5 min after contrast medium injection). During each phase, the CE US scanning was performed when the characteristic enhancement of focal liver lesions appeared.

Static 3D and Autosweep 3D functionalities, with which the LOGIQ 7 ultrasound imaging system is equipped, were used for image acquisition. Employing the different engineering features of these two functionalities, in the early phase, both Static 3D and Autosweep 3D were used to acquire 3D data, while in the two other phases only the Autosweep 3D functionality was used. A VOI with an adjustable scanning angle and size was determined before scanning to contain the desired region. The data acquired were stored as cineloops in the hard disk of the ultrasound imaging system.

Image reconstruction

3D image reconstruction was performed using the functionalities with which the LOGIQ 7 ultrasound system was equipped. In the VOI which was presented in an isotropic rectangular coordinate frame, the three orthogonal planes were referred to as plane A which could migrate from front to rear through the VOI, plane B from left to right and plane C from up to down. Tomographic ultrasound images (TUI) with presentation of several parallel slices in three orthogonal planes were reconstructed in three phases, while the number of slices that could be selected was 2, 4, or 6 for images obtained using Autosweep 3D, and 2, 4, or 9 for Static 3D. In

order to show the desired images, the range of distance between two slices in TUI could be adjusted if required. The mean times of these procedures were about 20 s. Sonographic angiogram images were reconstructed in an angio-like view during the early phase by using various rendering modes. The maximum intensity mode displaying the maximum grey values in the VOI, mixed with surface mode displaying the grey value on the surface of objects, was used to visualize tumor vessels and early tumor enhancement, while the average intensity mode displaying the average grey values in the VOI, mixed with surface mode, was employed to describe the tumor based on the predominantly unenhanced areas. The mean times of these procedures were about 45 s. TUI in three dimensions and sonographic angiogram images were stored with volume data in the hard disk of the ultrasound imaging system. In both the retrospective study and the prospective study, the reconstruction of all the images was completed by one operator with 10 years of experience in abdominal US and 1 year in CE 3D US, blinded to the final diagnosis and other related information on patients.

Image evaluation

Before the 3D image evaluations in both the retrospective and prospective studies, all readers were given training in the assessment of various enhancement patterns. Image evaluation was divided into two sections: in the first section, TUI in early, middle and late phases and sonographic angiograms in the early phase were reviewed separately in random order for all the lesions and the enhancement patterns in each phase were classified; in the second section, all images in three phases for each lesion were read consecutively to observe enhancement changes over time. In the prospective study, 2D images were read 2 wk after the 3D image review. All the images were reviewed on the ultrasound imaging system. The zoom function and arbitrary rotation of images are available in both TUI and sonographic angiograms.

In the retrospective study, images were reviewed independently by two readers (Numata K and Morimoto M) with 10 years of experience in liver US and 1.5 years of experience in CE 3D US imaging, who were blinded to final diagnosis and clinical and other radiological information. The readers were asked to classify the enhancement patterns in three phases and enhancement changes over time. In the early phase, the enhancement patterns consisted of tumor enhancement and tumor vessels: four tumor enhancement patterns including diffuse enhancement defined as homogeneous or heterogeneous tumor enhancement, peripheral ring-like enhancement defined as enhancement in the tumor periphery with a ring shape, peripheral nodular enhancement defined as enhancement in the tumor periphery with a nodular shape, and absence of tumor enhancement; four tumor vessel patterns including intratumoral vessels in the central portion of the tumor, peritumoral vessels at the periphery of the tumor, spoke-wheel arteries defined as a centrally located artery with centrifugal stellate branching, and absence of vessels. In the middle phase, four patterns were classified based on tumor enhancement: diffuse enhancement, peripheral ring-like enhancement, peripheral nodular enhancement and perfusion defect. In the late phase, the hypoechoic pattern was defined as all or part of the lesion having low echogenicity as compared to the surrounding liver parenchyma, and the isoechoic pattern as the entire lesion having echogenicity equal to that of the surrounding liver parenchyma. The enhancement changes over time were assessed: washout, early enhancement greater than that of the liver parenchyma and enhancement in the middle or late phase less than that of the liver parenchyma; persistence, whatever the enhancement pattern in the early phase was, enhancement of the lesion in the middle and late phases was at least equal to that of the liver parenchyma; absence of washout and persistence, no distinct enhancement was detected in any of the three phases.

Evaluations of 153 lesions by two readers were in concordance. For 10 lesions, enhancement patterns evaluated by two readers were different but a consensus was finally reached. After the pattern classification, the combination of enhancement patterns in the three phases was summarized and the positive predictive value (PPV) was calculated. The combined enhancement patterns with PPV more than 50% served as diagnostic criteria for the analysis in the prospective study.

In the prospective study, two readers (Nozaki A and Luo W) with 8 and 5 years of experience in CE US of the liver and 1 year of experience in CE 3D US imaging, blinded to the final diagnosis and clinical and other radiological information, read CE 3D US images and differentiated focal liver lesions according to the diagnostic criteria established in the retrospective study. After reading 2D images, these two readers also made a diagnosis of each lesion according to the criteria previously established (Table 2)[27,28,32,33].

On 3D images and 2D images, for each diagnosis, i.e. HCC, metastasis, hemangioma, and focal nodular hyperplasia (FNH), a four-point scale was used to grade diagnostic confidence. For instance, in HCCs, grade 1 was defined as "probably not a HCC lesion", grade 2 as "possibly not a HCC lesion", grade 3 as "possibly a HCC lesion" and grade 4 as "probably a HCC lesion". The confidence level of each reader was compared in consideration of the final diagnosis by two physicians (Kondo M and Tanaka K). True-positive (TP) cases were considered to be those assigned as grade 3 to 4 and verified by reference standards as actually being positive diagnoses. False-positive (FP) cases were considered to be those assigned as grade 3 to 4 but verified as actually being negative diagnoses. True-negative (TN) cases were considered to be those assigned as grade 1 to 2 by the reader, and verified as actually being negative diagnoses. False-negative (FN) cases were considered to be those assigned as grade 1 to 2 but verified as actually being positive diagnoses.

Table 2 Diagnostic criteria for focal liver lesions depicted by CE 2D US

Lesion	Enhancement patterns		
	Early phase	Middle phase	Late phase
HCC	Intratumoral vessels with early homogeneous or heterogeneous enhancement, or intratumoral vessels alone	Homogeneous or heterogeneous enhancement	Hypoechoic lesion
Metastasis	Peritumoral vessels with early peripheral ring like enhancement	Peripheral ring like enhancement or perfusion defect	Hypoechoic lesion
Hemangioma	Peripheral nodular enhancement	Peripheral nodular enhancement, with centripetal progression	Isoechoic lesion, with centripetal progression
FNH	Spoke-wheel arteries with early homogeneous enhancement	Homogeneous enhancement	Isoechoic lesion with central scar

CE: Contrast-enhanced; 2D US: Two-dimensional ultrasonography.

Statistical analysis

The data analysis was performed by using SPSS software (version 11.0; SPSS, Tokyo, Japan). In the retrospective study, SE was defined as the probability of the given enhancement pattern appearing in a reference disease, while SP indicated the probability of the absence of a given enhancement pattern for negative diagnoses. Prior probability was calculated by dividing the numbers of HCCs, metastases, hemangiomas and FNHs by the total number of tumors (163 tumors). According to Bayes theorem, the PPV of the combination of enhancement patterns for each tumor category was calculated based on sensitivity (SE), specificity (SP), and prior probability (PP) using the formula: PPV = SE × PP/[SE × PP + (1 - SP)× (1 - PP)].

In the prospective study, SE was calculated as TP/(TP + FN) and SP was calculated as TN/(FP + TN). The ROC curve was fitted to each reader's confidence level by using a maximum likelihood estimation program (ROCKIT 0.9B; http://www-radiology.uchicago.edu/krl/KRL_ROC). Area under the ROC curve (A_z) with the 95% confidential interval was calculated for each modality to measure the overall diagnostic performance. κ values were used to assess inter-reader agreement in characterizing focal liver tumors. Agreement was graded as poor (< 0.20), moderate (0.20 to 0.40), fair (0.40 to 0.60), good (0.60 to 0.80), or excellent (0.80 to 1.00).

RESULTS

Retrospective study

The enhancement patterns of 163 focal liver lesions are summarized in Table 3. In the early phase, 90% (88 of 98) of HCCs showed diffuse enhancement with intratumoral vessels (Figure 1A and B), 60% (21 of 35) of liver metastases peripheral ring-like enhancement with intratumoral or peritumoral vessels (Figure 2A), 79% (19 of 24) of hemangiomas peripheral nodular enhancement with peritumoral vessels or absence of vessels (Figure 3A and B), and 100% (6 of 6) of FNHs diffuse enhancement with spoke-wheel arteries (Figure 4A-C). In the middle phase, 93% (91 of 98) of HCCs showed diffuse enhancement (Figure 1C) and 69% (24 of 35) of metastases peripheral ring-like enhancement (Figure 2B), 75% (18 of 24) of hemangiomas peripheral nodular enhancement (Figure 3C) and 25% (6 of 24) diffuse enhancement, and 100% (6 of 6) of FNHs diffuse enhancement. In the late phase, 137 of 163 lesions were hypoechoic (Figures 1D, 2C, 2D and 3D), while the others were isoechoic (Figure 4D). Washout of enhancement was detected mainly in 121 of 133 malignant lesions (Figures 1 and 2), while enhancement persistence was detected mainly in 29 of 30 benign lesions (Figures 3 and 4). One HCC and two metastasis lesions were not enhanced from the early to the late phase and were assessed as showing absence of washout and persistence. The combination of enhancement patterns in three phases with PPV above 50% were summarized for each tumor category in Table 4 as the dominant enhancement patterns for establishing diagnostic criteria on 3D images in prospective study.

Prospective study

For CE 3D US, the diagnostic criteria for HCCs resulted in a SE of 93% (mean for two readers), SP of 91% and A_z value of 0.95, while those for metastases showed a SE of 84%, SP of 97% and A_z value of 0.95 in the prospective study. The combined enhancement patterns for hemangiomas as diagnostic criteria resulted in a SE of 91%, SP of 98% and A_z value of 0.98, while the dominant enhancement patterns for FNHs as diagnostic criteria resulted in a SE of 80%, SP of 99%, and A_z value of 0.99. Good to excellent inter-reader agreement was thus achieved for HCCs (κ = 0.86), metastases (κ = 0.83), hemangiomas (κ = 0.79) and FNHs (κ = 0.76).

For CE 2D US, sensitivity, specificity and A_z value of differential diagnosis were shown in Table 5. There were no significant differences between sensitivity, specificity and A_z value on CE 2D US and those on CE 3D US ($P > 0.05$). For HCCs, there was an SE of 92%, SP of 87% and A_z value of 0.95 (mean of two readers), while an SE of 84%, SP of 97% and A_z value of 0.94 were recorded for metastasis. For hemangioma, there was an SE of 84.5%, SP of 98% and A_z value of 0.95. For FNH, an SE of 70%, SP of 98% and A_z value of 0.98 were presented. SE, SP and A_z value of hemangioma and FNH on CE 2D US appeared lower than those on CE 3D US.

Table 3 Enhancement patterns using CE 3D US in three phases: positive predictive value in retrospective study

No.	Enhancement patterns					Positive predictive value			
	Early phase		Middle phase	Late phase	Enhancement changes	HCC	Metastasis	Hemangioma	FNH
	Tumor enhancement	Tumoral vessels	Tumor enhancement	Tumor echogenicity					
1	Diffuse	Intratumoral	Diffuse	Hypoechoic	Washout	0.98 (81)	0.01 (1)	0.01 (1)	0.00 (0)
2	Diffuse	Intratumoral	Diffuse	Isoechoic	Persistence	0.60 (3)	0.00 (0)	0.40 (2)	0.00 (0)
3	Diffuse	Intratumoral	Peripheral ring-like	Hypoechoic	Washout	0.33 (2)	0.67 (4)	0.00 (0)	0.00 (0)
4	Diffuse	Intratumoral	Perfusion defect	Hypoechoic	Washout	0.67 (2)	0.33 (1)	0.00 (0)	0.00 (0)
5	Diffuse	Spoke-wheel arteries	Diffuse	Isoechoic	Persistence	0.00 (0)	0.00 (0)	0.00 (0)	1.00 (6)
6	Peripheral ring-like enhancement	Intratumoral	Diffuse	Isoechoic	Persistence	1.00 (3)	0.00 (0)	0.00 (0)	0.00 (0)
7	Peripheral ring-like enhancement	Intratumoral	Peripheral ring-like	Hypoechoic	Washout	0.14 (1)	0.86 (6)	0.00 (0)	0.00 (0)
8	Peripheral ring-like enhancement	Peritumoral	Peripheral ring-like	Hypoechoic	Washout	0.00 (0)	1.00 (12)	0.00 (0)	0.00 (0)
9	Peripheral ring-like enhancement	Peritumoral	Perfusion defect	Hypoechoic	Washout	0.00 (0)	1.00 (3)	0.00 (0)	0.00 (0)
10	Peripheral nodular	Peritumoral	Diffuse	Isoechoic	Persistence	0.00 (0)	0.00 (0)	1.00 (1)	0.00 (0)
11	Peripheral nodular	Peritumoral	Peripheral nodular	Hypoechoic	Persistence	0.00 (0)	0.00 (0)	0.67 (2)	0.00 (0)
12	Peripheral nodular	Peritumoral	Peripheral nodular	Isoechoic	Persistence	0.00 (0)	0.00 (0)	1.00 (1)	0.00 (0)
13	Peripheral nodular	Peritumoral	Peripheral nodular	Hypoechoic	Washout	0.00 (0)	0.33 (1)	0.00 (0)	0.00 (0)
14	Peripheral nodular	Absence	Diffuse	Isoechoic	Persistence	0.00 (0)	0.00 (0)	1.00 (2)	0.00 (0)
15	Peripheral nodular	Absence	Peripheral nodular	Hypoechoic	Persistence	0.00 (0)	0.00 (0)	1.00 (8)	0.00 (0)
16	Peripheral nodular	Absence	Peripheral nodular	Isoechoic	Persistence	0.00 (0)	0.00 (0)	1.00 (5)	0.00 (0)
17	Absence	Intratumoral	Diffuse	Isoechoic	Persistence	1.00 (3)	0.00 (0)	0.00 (0)	0.00 (0)
18	Absence	Intratumoral	Diffuse	Hypoechoic	Washout	1.00 (1)	0.00 (0)	0.00 (0)	0.00 (0)
19	Absence	Intratumoral	Peripheral ring-like	Hypoechoic	Washout	0.00 (0)	1.00 (1)	0.00 (0)	0.00 (0)
20	Absence	Intratumoral	Perfusion defect	Hypoechoic	Washout	1.00 (1)	0.00 (0)	0.00 (0)	0.00 (0)
21	Absence	Peritumoral	Peripheral ring-like	Hypoechoic	Washout	0.00 (0)	1 .00(1)	0.00 (0)	0.00 (0)
22	Absence	Peritumoral	Perfusion defect	Hypoechoic	Washout	0.00 (0)	1.00 (3)	0.00 (0)	0.00 (0)
23	Absence	Absence	Perfusion defect	Hypoechoic	Absence	0.33 (1)	0.67 (2)	0.00 (0)	0.00 (0)
24	Absence	Absence	Peripheral nodular	Hypoechoic	Persistence	0.00 (0)	0.00 (0)	1.00 (2)	0.00 (0)

Positive predictive values are presented with number of lesions in parentheses.

Table 4 Sensitivity, specificity and A_z value for differential diagnosis based on CE 3D US in prospective study

Focal liver tumors	Diagnostic criteria based on combined enhancement patterns		Sensitivity	Specificity	A_z value
HCC	1, 2, 4, 6, 17, 18, 20	Reader 1	91 (64/70)	90 (44/49)	0.94 (0.88-0.95)
		Reader 2	94 (66/70)	92 (45/49)	0.96 (0.91-0.98)
Metastasis	3, 7, 8, 9, 13, 19, 21, 22, 23	Reader 1	86 (24/28)	97 (88/91)	0.95 (0.89-0.98)
		Reader 2	82 (23/28)	96 (87/91)	0.94 (0.89-0.97)
Hemangioma	10, 11, 12, 14, 15, 16, 24	Reader 1	94 (15/16)	98 (101/103)	0.98 (0.94-1.00)
		Reader 2	88 (14/16)	97 (100/103)	0.97 (0.90-1.00)
FNH	5	Reader 1	80 (4/5)	98 (112/114)	0.99 (0.95-1.00)
		Reader 2	80 (4/5)	99 (113/114)	0.98 (0.87-1.00)

Combined enhancement patterns for diagnostic criteria are summarized according to the serial numbers in Table 3. Sensitivity and specificity data are presented as percentages with numbers of tumors in parentheses, and A_z values are presented with 95% confidence intervals in parentheses.

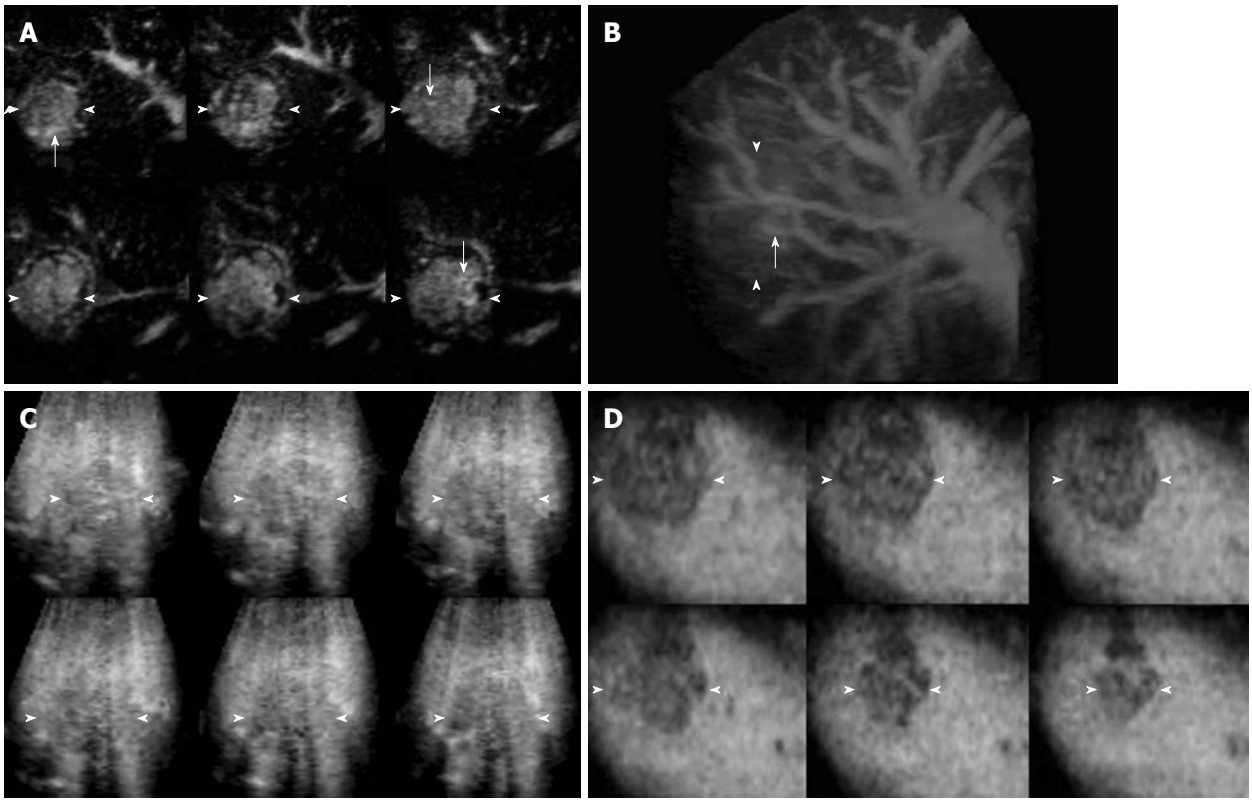

Figure 1 Contrast-enhanced (CE) three-dimensional ultrasonography (3D US) images of the liver in a 57-year-old man with hepatocellular carcinoma (HCC) in the anterior superior segment of the right lobe. A, B: Tomographic ultrasound image with slice distance 1.5 mm in plane A (A) and the sonographic angiogram rendered by maximum intensity with surface mode (B) show diffuse enhancement with intratumoral vessels (arrows) in the early phase; C: Tomographic ultrasound image with slice distance 2.0 mm in plane B shows diffuse enhancement in the middle phase; D: Tomographic ultrasound image with slice distance 2.0 mm in plane C shows hypoechoic pattern in the late phase. Enhancement change of washout was detected in this lesion. Arrowheads indicate the tumor margin.

Table 5 Sensitivity, specificity and A_z value for differential diagnosis based on CE 2D US in prospective study

Lesion	Sensitivity	Specificity	A_z value (95% CI)
HCC			
Reader 1	89 (62/70)	88 (43/49)	0.95 (0.89-0.98)
Reader 2	94 (66/70)	86 (42/49)	0.95 (0.90-0.98)
Metastasis			
Reader 1	86 (24/28)	96 (87/91)	0.93 (0.85-0.97)
Reader 2	82 (23/28)	98 (89/91)	0.95 (0.88-0.98)
Hemangioma			
Reader 1	81 (13/16)	97 (100/103)	0.94 (0.80-0.99)
Reader 2	88 (14/16)	99 (102/103)	0.95 (0.73-1.00)
FNH			
Reader 1	60 (3/5)	97 (111/114)	0.97 (0.74-1.00)
Reader 2	80 (4/5)	98 (112/114)	0.98 (0.66-1.00)

Sensitivity and specificity data are presented as percentages with numbers of tumors in parentheses.

DISCUSSION

Our study explored the potential role of CE 3D US, a newly-developed imaging modality, in presenting various tumor enhancement patterns and further characterizing different types of focal liver lesions. In this study, we used Sonazoid with CHA mode and high mechanical index contrast conditions, which allowed sensitive observation of vessels in the early phase by eliminating microbubbles in microvessels but not those in relatively large vessels, such as tumor vessels and portal veins[19].

In a previous study, we explored the visualization methods of CE 3D US for demonstrating focal liver lesions[24]. Moreover, in a retrospective study, according to the diagnostic criteria based on our experience and that described in the literatures, we assessed the diagnostic value of CE 3D US for characterization of focal liver lesions, in comparison with that of CE 3D CT[22]. Further, in the present study, we performed a retrospective study to clarify the enhanced patterns of focal liver lesions on CE 3D US, and the combined enhancement patterns with PPV more than 50% served as diagnostic criteria. According to these diagnostic criteria, we prospectively evaluated CE 3D US for characterizing liver lesions.

On CE 3D US, sonographic angiograms rendered using maximum intensity mode could be used to delineate tumor enhancement and present the spatial distribution of tumor vessels. Spoke-wheel arteries were regarded as a typical characteristic of FNHs on CE imaging in previous studies[34-36]. CE 3D US facilitated categorization of spoke-wheel arteries and provided a tridimensional view of the stellate branches. With consensus of the two readers, all 6 FNHs in the retrospective study were detected based on spoke-wheel arteries followed by persistent enhancement. In the prospective study, except for one FNH without distinctly detectable of spoke-wheel arteries, 4 of the other 5

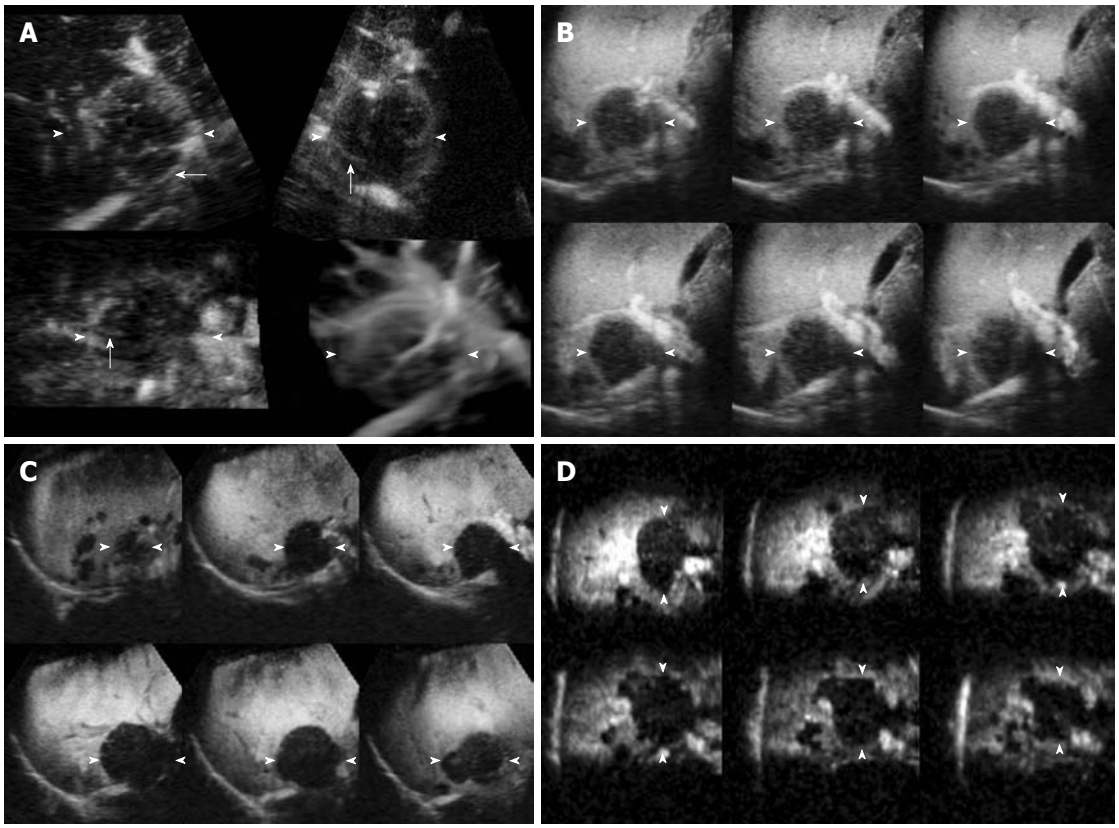

Figure 2 CE 3D US images of the liver in a 64-year-old woman with metastases from pancreatic carcinoma in the anterior superior segment of the right lobe. A: Images in the early phase show peripheral ring-like enhancement with peritumoral vessels (arrows) in plane A (upper left), plane B (upper right), plane C (lower left) and the sonographic angiogram rendered by average intensity with surface mode (lower right); B: Tomographic ultrasound image with slice distance 2.0 mm in plane A shows peripheral ring-like enhancement in the middle phase; C, D: Tomographic ultrasound images (TUI) in plane A with slice distance 2.5 mm (C) and that in plane C with slice distance 2.0 mm (D) show hypoechoic pattern in the late phase. Enhancement change of washout was detected in this lesion. Arrowheads indicate the tumor margin.

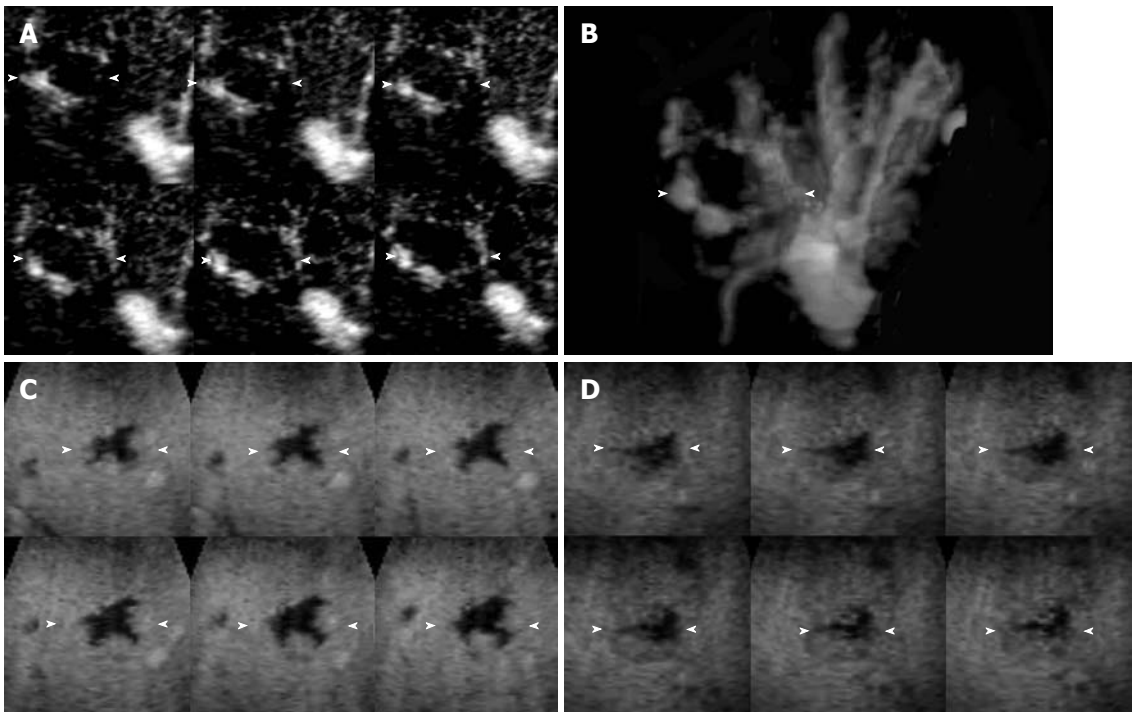

Figure 3 CE 3D US images of the liver in a 59-year-old woman with a hemangioma in the anterior inferior segment of the right lobe. A, B: Tomographic ultrasound image in plane A with slice distance 1.0 mm (A) and sonographic angiogram rendered by average intensity with surface mode (B) show peripheral nodular enhancement without distinct tumor vessels in the early phase; C: Tomographic ultrasound image in plane B with slice distance 1.0 mm shows peripheral nodular enhancement in the middle phase; D: Tomographic ultrasound image with slice distance 1.0 mm in plane B with slice distance 1.0 mm shows hypoechoic pattern in the late phase. Persistent enhancement over time was detected in this lesion. Arrowheads indicate the tumor margin.

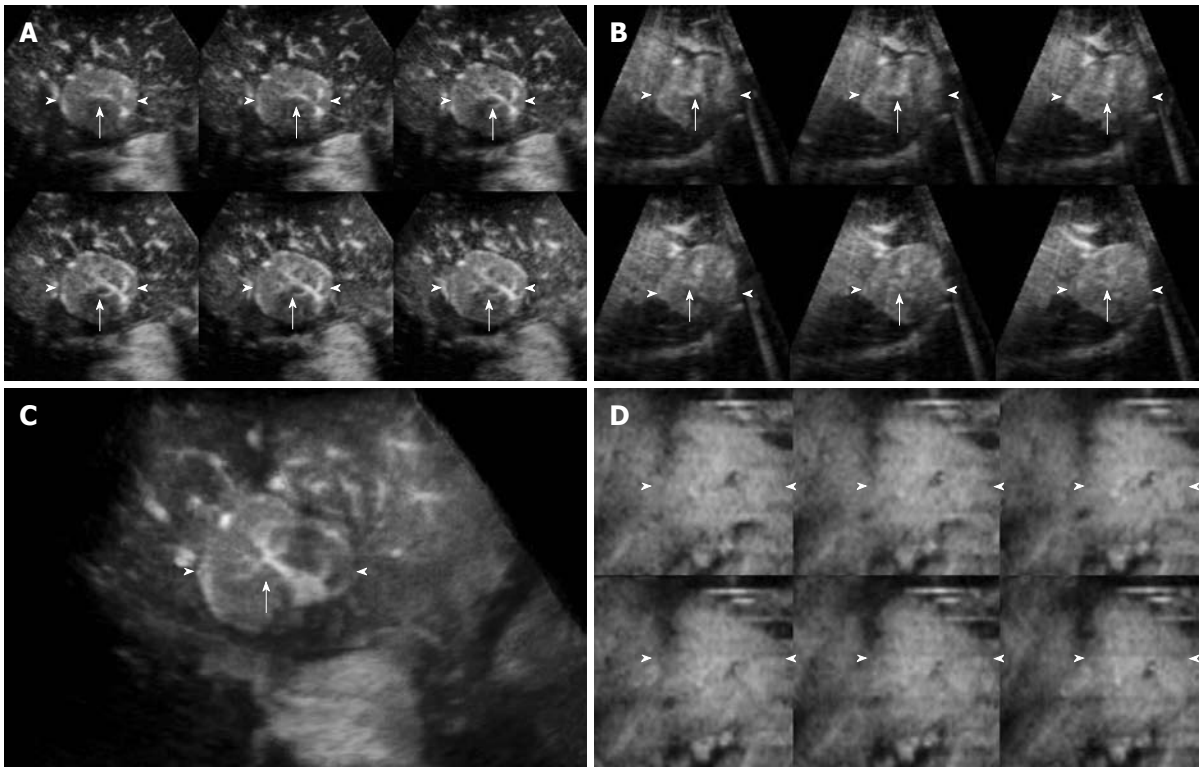

Figure 4 CE 3D US images of the liver in a 77-year-old man with FNH in the medial segment of the left lobe. A-C: TUI in plane A with slice distance 1.5 mm (A) and plane B with slice distance 1.5 mm (B), and the sonographic angiogram rendered by maximum intensity with surface mode (C) show diffuse enhancement with spoke-wheel arteries (arrows) in the early phase; D: TUI in plane C with slice distance 2.5 mm show isoechoic pattern in the late phase and hypoechoic regions within the tumor indicate central scars. Persistent enhancement over time was detected in this lesion. Arrowheads indicate the tumor margin.

lesions were diagnosed correctly. For the lesions with peripheral enhancement, sonographic angiograms rendered using average intensity modes delineated unenhanced portions in the lesions with hypoechoic appearance to make the tumor distinguishable from the surrounding liver parenchyma. Another feature of CE 3D US was the application of tomographic images presented in several parallel slices to multiplanar reconstruction, which allowed the reader to evaluate enhancement patterns in different portions of the lesion simultaneously. In this study, although there were no significant differences between the prospective diagnosis at CE 3D US and that at CE 2D US, CE 3D US created a spatial and easily understood view for both hemodynamic and morphologic evaluation of focal liver tumors, which were formed only in the doctors' imagination by 2D imaging using complex acquisition methods. The good to excellent inter-reader agreement in our previous study about CE 3D US as a means of presenting characteristic enhancement of HCCs has indicated CE 3D US can exhibit the characteristic enhancement of HCC tumors objectively[34].

In the present study, with analysis of combination of the enhancement in three phases at CE 3D US, the dominant patterns were used as the diagnostic criteria for individual category, and prospective differentiation yielded a good sensitivity, specificity, high A_z value, and good to excellent inter-reader agreement, which revealed the potential usage of CE 3D US in differentiating various focal liver lesions.

In the late phase in the retrospective study, 91% of malignant tumors (88 HCCs and 33 metastases) with washout changes appeared hypoechoic, while 53% of benign tumors (10 hemangiomas and 6 FNHs) with persistent enhancement appeared isoechoic. Neither isoechoic metastases nor hypoechoic FNHs were found in the late phase. There were 13 hemangiomas exhibiting hypoechoic findings in the late phase, and 12 of these 13 lesions were detected with incomplete fill-in and persistent enhancement, while one hemangioma was detected with early diffuse enhancement and washout change and was confirmed by the histological results on surgery. Vascularity in the early and middle phases appeared to be important for differentiation of focal liver lesions, and enhancement in the late phase with enhancement changes over time also facilitated characterizing the benign and malignant lesions[28,37].

This study has some limitations. First, CE 3D US on focal liver lesions has shortcomings including artifacts from the heart or respiratory motion, shadows of costal bones, and interference from abdominal gas, and so on. We minimized the influence of artifacts by requiring patients to hold their breath during the scanning procedure, selecting the location of the volume transducer, mediating the size and position of VOI, adjusting the scanning angle, and reconstructing the sonographic angiogram with appropriate rendering modes. Nevertheless, in some cases, artifacts on CE 3D US images might impact the readers' judgments and these lesions were thus excluded.

Second, in each case, only one lesion was evaluated and we did not assess the diagnostic capability and detectability of multiple lesions with CE 3D US. Third, the FNH cases in this study were few because FNHs have a relatively low prevalence and Sonazoid has been available in Japan for less than 2 years. More cases need to be examined in a future investigation.

In summary, our present results indicate CE 3D US with the contrast agent Sonazoid to offer a novel and useful means of presenting the vascularity characteristics three-dimensionally and differentiation of focal liver lesions with good diagnostic capability. These features of CE 3D US are anticipated to be of benefit in clinical diagnosis.

COMMENTS

Background

Recently, contrast-enhanced (CE) ultrasound (US) appeared as an important modality to show the vascularity in the areas of interest, and has been used widely in clinical diagnosis of liver lesions. Three dimensional ultrasonography (3D US) allows three orthogonal planes to spatially demonstrate the features of subjects, which has been frequently used in fetal US. Different from the 2D images, CE 3D US acquires the data in a volume of interest (VOI) by automatically scanning with a desired angle and allows reconstruction of tomographic images in three orthogonal planes and renders angiogram-like images. The combination of 3D US and CE US can present the enhancement of lesions in three dimensions and also in parallel slices by multiple- planar visualization.

Research frontiers

With the advantages of non-invasiveness, no radiation and flexible operation, CE US has become increasingly important in the detection and characterization of focal liver tumors over the past several years. Sonazoid (Daiichi Sankyo, Tokyo, Japan), a newly-developed second-generation US contrast agent, which consists of microbubbles (mean diameter 2-3 μm) of a perfluorobutane gas stabilized by a phospholipid monolayer shell, allows continuous real-time CE imaging for more than 10 min, and improves the reproducibility and durability of CE US examination.

Innovations and breakthroughs

To the authors' knowledge, although many studies on differentiation among various focal liver tumors have been conducted using CE 2D US and recently a few using CE 2D US with Sonazoid, the exact value of CE 3D US with Sonazoid in the differential diagnosis of various focal liver tumors has not yet been clarified. Thus, in this study, in order to examine the potential role of CE 3D US in characterizing focal liver tumors, the authors retrospectively evaluated tumor enhancement patterns, and the diagnostic criteria established using dominant enhancement patterns were then applied to differentiation among focal liver tumors in a prospective study.

Applications

The study's results suggest that CE 3D ultrasound provides a spatial perspective for liver tumor enhancement, and could help in differentiating focal liver tumors.

Terminology

Contrast enhanced ultrasound: the imaging modality of using US scanning while microbubbles serving as contrast agent are injected into vessels in order to improve the signals of red blood cells. Using this modality, the vascularity of VOI was depicted exactly and hemodynamics was demonstrated clearly.

Peer review

The aim of this study is to differentiate focal liver lesions based on enhancement patterns using 3D US with perflubutane-based contrast agent. The paper is written in a good English form, and is properly structured.

REFERENCES

1 **Hamer OW**, Schlottmann K, Sirlin CB, Feuerbach S. Technology insight: advances in liver imaging. *Nat Clin Pract Gastroenterol Hepatol* 2007; **4**: 215-228

2 **Pandharipande PV**, Krinsky GA, Rusinek H, Lee VS. Perfusion imaging of the liver: current challenges and future goals. *Radiology* 2005; **234**: 661-673

3 **Bilgili Y**, Firat Z, Pamuklar E, Unal B, Hyslop W, Rivero H, Semelka RC. Focal liver lesions evaluated by MR imaging. *Diagn Interv Radiol* 2006; **12**: 129-135

4 **Tchelepi H**, Ralls PW. Ultrasound of focal liver masses. *Ultrasound Q* 2004; **20**: 155-169

5 **Hori M**, Murakami T, Kim T, Tomoda K, Nakamura H. CT Scan and MRI in the Differentiation of Liver Tumors. *Dig Dis* 2004; **22**: 39-55

6 **Rettenbacher T**. Focal liver lesions: role of contrast-enhanced ultrasound. *Eur J Radiol* 2007; **64**: 173-182

7 **Dietrich CF**. Characterisation of focal liver lesions with contrast enhanced ultrasonography. *Eur J Radiol* 2004; **51** Suppl: S9-S17

8 **Konopke R**, Bunk A, Kersting S. The role of contrast-enhanced ultrasound for focal liver lesion detection: an overview. *Ultrasound Med Biol* 2007; **33**: 1515-1526

9 **Quaia E**, Calliada F, Bertolotto M, Rossi S, Garioni L, Rosa L, Pozzi-Mucelli R. Characterization of focal liver lesions with contrast-specific US modes and a sulfur hexafluoride-filled microbubble contrast agent: diagnostic performance and confidence. *Radiology* 2004; **232**: 420-430

10 **Wen YL**, Kudo M, Zheng RQ, Ding H, Zhou P, Minami Y, Chung H, Kitano M, Kawasaki T, Maekawa K. Characterization of hepatic tumors: value of contrast-enhanced coded phase-inversion harmonic angio. *AJR Am J Roentgenol* 2004; **182**: 1019-1026

11 **Claudon M**, Cosgrove D, Albrecht T, Bolondi L, Bosio M, Calliada F, Correas JM, Darge K, Dietrich C, D'Onofrio M, Evans DH, Filice C, Greiner L, Jäger K, Jong N, Leen E, Lencioni R, Lindsell D, Martegani A, Meairs S, Nolsøe C, Piscaglia F, Ricci P, Seidel G, Skjoldbye B, Solbiati L, Thorelius L, Tranquart F, Weskott HP, Whittingham T. Guidelines and good clinical practice recommendations for contrast enhanced ultrasound (CEUS) - update 2008. *Ultraschall Med* 2008; **29**: 28-44

12 **D'Onofrio M**, Rozzanigo U, Masinielli BM, Caffarri S, Zogno A, Malagò R, Procacci C. Hypoechoic focal liver lesions: characterization with contrast enhanced ultrasonography. *J Clin Ultrasound* 2005; **33**: 164-172

13 **D'Onofrio M**, Rozzanigo U, Caffarri S, Zogno A, Procacci C. Contrast-enhanced US of hepatocellular carcinoma. *Radiol Med* 2004; **107**: 293-303

14 **Brannigan M**, Burns PN, Wilson SR. Blood flow patterns in focal liver lesions at microbubble-enhanced US. *Radiographics* 2004; **24**: 921-935

15 **Quaia E**. Microbubble ultrasound contrast agents: an update. *Eur Radiol* 2007; **17**: 1995-2008

16 **Yanagisawa K**, Moriyasu F, Miyahara T, Yuki M, Iijima H. Phagocytosis of ultrasound contrast agent microbubbles by Kupffer cells. *Ultrasound Med Biol* 2007; **33**: 318-325

17 **Watanabe R**, Matsumura M, Chen CJ, Kaneda Y, Fujimaki M. Characterization of tumor imaging with microbubble-based ultrasound contrast agent, sonazoid, in rabbit liver. *Biol Pharm Bull* 2005; **28**: 972-977

18 **Sontum PC**. Physicochemical characteristics of Sonazoid, a new contrast agent for ultrasound imaging. *Ultrasound Med Biol* 2008; **34**: 824-833

19 **Numata K**, Morimoto M, Ogura T, Sugimori K, Takebayashi S, Okada M, Tanaka K. Ablation therapy guided by contrast-enhanced sonography with Sonazoid for hepatocellular carcinoma lesions not detected by conventional sonography. *J Ultrasound Med* 2008; **27**: 395-406

20 **Nakano H**, Ishida Y, Hatakeyama T, Sakuraba K, Hayashi M, Sakurai O, Hataya K. Contrast-enhanced intraoperative ultrasonography equipped with late Kupffer-phase image obtained by sonazoid in patients with colorectal liver metas-

tases. *World J Gastroenterol* 2008; **14**: 3207-3211
21 **Dietrich CF**. [3D real time contrast enhanced ultrasonography, a new technique] *Rofo* 2002; **174**: 160-163
22 **Luo W**, Numata K, Morimoto M, Kondo M, Takebayashi S, Okada M, Morita S, Tanaka K. Focal liver tumors: characterization with 3D perflubutane microbubble contrast agent-enhanced US versus 3D contrast-enhanced multidetector CT. *Radiology* 2009; **251**: 287-295
23 **Forsberg F**, Goldberg BB, Merritt CR, Parker L, Maitino AJ, Palazzo JJ, Merton DA, Schultz SM, Needleman L. Diagnosing breast lesions with contrast-enhanced 3-dimensional power Doppler imaging. *J Ultrasound Med* 2004; **23**: 173-182
24 **Luo W**, Numata K, Morimoto M, Nozaki A, Nagano Y, Sugimori K, Tanaka K. Three-dimensional contrast-enhanced sonography of vascular patterns of focal liver tumors: pilot study of visualization methods. *AJR Am J Roentgenol* 2009; **192**: 165-173
25 **Ohto M**, Kato H, Tsujii H, Maruyama H, Matsutani S, Yamagata H. Vascular flow patterns of hepatic tumors in contrast-enhanced 3-dimensional fusion ultrasonography using plane shift and opacity control modes. *J Ultrasound Med* 2005; **24**: 49-57
26 **Yukisawa S**, Ohto M, Masuya Y, Okabe S, Fukuda H, Yoshikawa M, Ebara M, Saisho H, Ohtsuka M, Miyazaki M, Kondo F. Contrast-enhanced three-dimensional fusion sonography of small liver metastases with pathologic correlation. *J Clin Ultrasound* 2007; **35**: 1-8
27 **Isozaki T**, Numata K, Kiba T, Hara K, Morimoto M, Sakaguchi T, Sekihara H, Kubota T, Shimada H, Morizane T, Tanaka K. Differential diagnosis of hepatic tumors by using contrast enhancement patterns at US. *Radiology* 2003; **229**: 798-805
28 **Nicolau C**, Vilana R, Catalá V, Bianchi L, Gilabert R, García A, Brú C. Importance of evaluating all vascular phases on contrast-enhanced sonography in the differentiation of benign from malignant focal liver lesions. *AJR Am J Roentgenol* 2006; **186**: 158-167
29 **Burns PN**, Wilson SR. Focal liver masses: enhancement patterns on contrast-enhanced images--concordance of US scans with CT scans and MR images. *Radiology* 2007; **242**: 162-174
30 **Hatanaka K**, Kudo M, Minami Y, Ueda T, Tatsumi C, Kitai S, Takahashi S, Inoue T, Hagiwara S, Chung H, Ueshima K, Maekawa K. Differential diagnosis of hepatic tumors: value of contrast-enhanced harmonic sonography using the newly developed contrast agent, Sonazoid. *Intervirology* 2008; **51** Suppl 1: 61-69
31 **Bruix J**, Sherman M. Management of hepatocellular carcinoma. *Hepatology* 2005; **42**: 1208-1236
32 **Numata K**, Isozaki T, Morimoto M, Sugimori K, Kunisaki R, Morizane T, Tanaka K. Prospective study of differential diagnosis of hepatic tumors by pattern-based classification of contrast-enhanced sonography. *World J Gastroenterol* 2006; **12**: 6290-6298
33 **Dill-Macky MJ**, Burns PN, Khalili K, Wilson SR. Focal hepatic masses: enhancement patterns with SH U 508A and pulse-inversion US. *Radiology* 2002; **222**: 95-102
34 **Vilgrain V**. Focal nodular hyperplasia. *Eur J Radiol* 2006; **58**: 236-245
35 **Ungermann L**, Eliás P, Zizka J, Ryska P, Klzo L. Focal nodular hyperplasia: spoke-wheel arterial pattern and other signs on dynamic contrast-enhanced ultrasonography. *Eur J Radiol* 2007; **63**: 290-294
36 **Yen YH**, Wang JH, Lu SN, Chen TY, Changchien CS, Chen CH, Hung CH, Lee CM. Contrast-enhanced ultrasonographic spoke-wheel sign in hepatic focal nodular hyperplasia. *Eur J Radiol* 2006; **60**: 439-444
37 **Luo W**, Numata K, Morimoto M, Nozaki A, Nagano Y, Sugimori K, Zhou X, Tanaka K. Clinical utility of contrast-enhanced three-dimensional ultrasound imaging with Sonazoid: findings on hepatocellular carcinoma lesions. *Eur J Radiol* 2009; **72**: 425-431

S- Editor Wang JL **L- Editor** O'Neill M **E- Editor** Zheng XM